Proceedings of the ASME 2017 Dynamic Systems and Control Conference
DSCC2017
October 11-13, 2017, Tysons, Virginia, USA

DSCC2017-5234

PLACING MINIMUM PHASE ZEROS TO SHAPE TRANSIENT RESPONSE: GENERALIZATION FROM CONTROL OF HYBRID POWER SYSTEMS

Bilal S. Salih *
Department of Mech. and Aerospace Engineering
University of Central Florida
Orlando, Florida 32816
Email: Bilal.salih@knights.ucf.edu

Tuhin K. Das
Department of Mech. and Aerospace Engineering
University of Central Florida
Orlando, Florida 32816
Email: tuhin.das@ucf.edu

ABSTRACT

Conservation of energy can be applied in designing control of hybrid power systems to manage power demand and supply. In practice, it can be used for designing decentralized controllers. In this paper, this idea is analyzed in a generalized theoretical framework. The problem is transformed to that of using minimum phase zeros to generate a specific type of transient response admitted by dynamical systems. Here, the transient step response is shaped using an underlying conservation principle. In this paper, emphasis is placed on second order systems. However, the analysis can be extended to higher order transfer functions. Analytical results relating zero location to the matched/ mismatched areas of the transient response are established for a class of second order systems. A combination of feedback and feedforward actions are shown to achieve the desired zero placement/addition and the desired transient response. The proposed analysis promises extension to nonlinear systems. Optimization studies also seem appropriate, especially for higher order transfer functions.

INTRODUCTION

Hybrid Power Systems (*HPS*) are a combination of diversified modes of energy generation technologies, both renewable and non-renewable. *HPS* augment flexibility of power generation sources by optimizing the utilization, and balancing the strengths and shortages of each source [1, 2]. Solid oxide fuel cells (*SOFC*) combined with gas turbines or wind turbines (*WT*)combined with solar dishes and battery storage are examples of *HPS*. A thorough review of such systems and other examples can be found in [3, 4]. Strengthening *HPS* with an Energy Storage Device (*ESD*) could improve efficiency significantly. The integration of *ESD* in *HPS* ensures maintaining an instantaneous power demand when it exceeds the maximum power supplied by the system [1]. Ultra-capacitor (*UC*) is dominantly used, solo or in combination with $Li-ion$ battery, in order to augment *HPS* performance and improve load following capability. This is due to its ability of being charged or discharged quickly without degradation or damaging the cell [5]. In order to integrate *UC* in *HPS*, a control strategy and power management algorithm are required to safeguard the storage device from being overcharged or progressively discharged. Robust control strategies for a *SOFC* system with *UC*, based on nonlinear and H∞ control applications, were introduced in [6, 7]. The core of the aforementioned strategies is to have a central processor that receives locally sensed information and controls all the components of the *HPS*. Such a scheme is referred to as a centralized power management control. Although a centralized control approach is easier to be developed, its implementation can encounter practical limitations such as system scalability. Another drawback is that any failure in the central processor will crucially affect the functionality of the entire system [8]. In contrast, decentralization solves the issue of scalability and provides a remedy for the practical limitations mentioned above. Research investigations of decentralized control strategies of power systems can be found in [9–11].

In prior work, addressed in [12], one of the authors of this study proposed a decentralized power management for *HPS*. The system consists of a power source *SOFC* connected in parallel to a storage device *UC*. While the load demand is being met by the *HPS*, the proposed power management approach applies energy conservation principles to assure that the total energy of the *UC* remains constant after the charge/discharge cycles. Individual controllers for the power source and storage device are developed as follows: The power source controller utilizes its own transient response history to anticipate the energy deficit that is recovered by the storage device, and accordingly, alter its own output power. In the meantime, the second controller enables the *UC* to work as an energy buffer and track the load in the presence of fluctuating load demand. The following research is motivated by the observation that energy conservation principles

*Address all correspondence to this author.

can be applied to develop decentralized controllers of *HPS*. In this context, a theoretical framework study is conducted to further explore this idea. The characterizations of which a system response should have to maintain energy conservation requirements are investigated. In this regard, a formulation based on area-matching is proposed. Fundamentally, the goal is to obtain the overall transfer function a system should posses to generate area-matching transient. Here, the dynamic response of the system will result in a shape for which the summation of areas above and areas below a constant reference will be matched/ mismatched. Therefore, the response of the first and second order systems will be examined. As a result, a modified second order system model that assures area-matching will be formulated. A combination of feedback and feedforward actions will be used to achieve the desired transient response. Furthermore, the necessity of adding/placing a proper minimum phase zero in such a system will be confirmed. Analytical results relating the zero location to the aforementioned matched/mismatched areas will be also presented. The proposed analysis can help generalize the concept of area-matching transient to higher order linear and nonlinear systems and optimal control. In addition, this investigation can provide a path for more studies in the area of feedforward controls and the affect of system zero placement/ addition. The direct application of our research is the power management of *HPS*, as illustrated in the aforementioned discussion. The applicability of this approach in the area of the rendezvous / pursuit problems is also worth studying.

In this paper, theoretical analysis to demonstrate the concept of area-matching transient is first presented. Then, the conditions under which a second order system can maintain area-matching are obtained and discussed. Next, observations are addressed. Finally a conclusion is provided.

1 AREA-MATCHING TRANSIENTS

1.1 Example Motivated by Energy Conservation Based Control of *HPS*

Applying conservation of energy in designing control of *HPS* to manage power demand and supply, and to handle *ESD*, was proposed by one of the authors of this study in [12]. The concept of this idea is demonstrated in Fig. 1 and shows the load following mode response of a *HPS*. The response X_{RL} represents a step change in load demand that should be supplied by the *HPS*, and X_{RS} represents the corresponding response of the primary power source of the system. The interval $t_s \leq t \leq t_f$ represents the transient region as the response X_{RS} continues tracking the changing load demand X_{RL}, matching it at a steady state, $t > t_f$. In order to avoid the fluctuation in delivered power during the transient interval, the *ESD* works as a buffer that delivers the power demand and absorbs the extra energy provided by the primary power source. Therefore, the primary power source should provide enough energy to maintain the load demand and compensate the energy removed from the *ESD* during the transient response. In addition, the energy of the *ESD* should be preserved in order from being overcharged while the load demand is being met. A detailed explanation is presented in Fig. 1. The unshaded areas underneath X_{RL}, denoted by $A_{b,i}$, represent the gap between the provided energy from the primary power source and the load demand ; i.e. the amount of energy discharged from the *ESD*. Similarly, the unshaded areas above X_{RL}, denoted by $A_{a,j}$, represent the extra energy to be supplied by the primary power source in order to maintain the load demand and charge the *ESD*. Hence, the condition

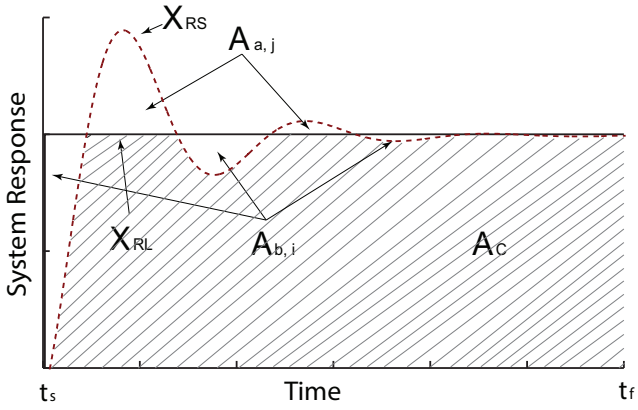

FIGURE 1. AREA MATCHING TRANSIENT

$$\lim_{t\to\infty}\left[\sum_{i=1} A_{b,i} - \eta \sum_{j=1} A_{a,j}\right] \to 0 \tag{1}$$

will ensure that the energy of the *ESD* is preserved while the load demand is being met. The presence of system losses during the charge / discharge cycles is defined through the efficiency η. Generalizing the result from Eqn. (1) for linear second order system is addressed in the next section.

1.2 Generalized Problem Formulation

In this research study, our goal is to investigate which characteristics, a transient response of a system should have in order to provide a behavior that can maintain energy conservation requirements. Conceptually, the objective is to propose control solutions that can shape the response of the system in a form for which the difference between $\sum_{i=1}^{\infty} A_{b,i}$ and $\sum_{j=1}^{\infty} A_{a,j}$ equals a targeted value η. Ideally when losses are absent, i.e. $\eta = 1$, the difference equals zero because the above and below areas cancel each other. We refer to this approach by area-matching transient analysis. Similar terminology, known as equal area criterion, can be found in literature [13–15]. However, the fundamental of the two approaches is different. The equal area criterion is related to the phase synchronization problem in AC power supplies with mutable sources. On the other hand, the analysis of area-matching, proposed in this work, provides a control strategy to modify system characteristics through controlled parameters as required. In order to generalize the discussion and formulate the problem, let A_{RS}, A_{RL}, and A_C be the area underneath the curve

X_{RS}, the area underneath the reference line X_{RL}, and the common area under X_{RL} and X_{RS}, respectively, as shown in Fig. 1. Consequently, expressions for A_{RS} and A_{RL} can be formulated as follows:

$$A_{RL} = A_C + \sum_{i=1}^{\infty} A_{b,i}, \quad A_{RS} = A_C + \sum_{j=1}^{\infty} A_{a,j} \tag{2}$$

Upon adding A_C to both sides of the desired Eqn. (1) and applying the expressions from Eqn. (2),

$$\begin{aligned} A_C + \textstyle\sum_{i=1}^{\infty} A_{b,i} &= A_C + \eta \textstyle\sum_{j=1}^{\infty} A_{a,j} \\ \implies A_{RL} &= [A_{RS} - \textstyle\sum_{j=1}^{\infty} A_{a,j}] + \eta \textstyle\sum_{j=1}^{\infty} A_{a,j} \end{aligned} \tag{3}$$

Eqn. (3) then can be simplified as:

$$A_{RS} - A_{RL} = [1-\eta] \sum_{j=1}^{\infty} A_{a,j} \tag{4}$$

The result from Eqn. (4) represents the condition that must be satisfied to ensure the applicability of the area-matching transient which is addressed in the next section.

2 A CLASS OF SECOND ORDER SYSTEMS WITH MINIMUM PHASE ZEROS

The response of first order system does not exhibit the oscillatory behavior that is essential for area-matching transient. Thus, we begin by exploring the response of a pure second order system that has only poles with no zeros as shown below:

$$\ddot{X} + 2\zeta\omega_n \dot{X} + {\omega_n}^2 X = {\omega_n}^2 u(t) \tag{5}$$

where ζ and ω_n are the damping ratio and the natural frequency, respectively. However, Eqn. (4) can not be satisfied by a system with a pure second order dynamic as shown in the next calculations. Eqn. (6) shows the under-damped step response of the system presented in Eqn. (5)

$$X(t) = 1 - \exp^{-\sigma t}\left[\cos\omega_d t + \frac{\sigma}{\omega_d}\sin\omega_d t\right] \tag{6}$$

where $\sigma = \zeta\omega_n$ and $\omega_d = \omega_n\sqrt{1-\zeta^2}$. Referring to Fig. 1, let X_{RS} be the unit step response from Eqn. (6), that is $X_{RS} = X(t)$. In addition, let X_{RL} be a unit step reference line, i.e. $X_{RL} = 1(t)$. In order to satisfy the condition from Eqn. (4) with the absence of losses, $\eta = 1$, the ramp error e_{ramp} of Eqn. (6) should approach zero as follows:

$$A_{RS} - A_{RL} = -e_{ramp} = \lim_{t\to\infty}\left[\int_0^t X_{RS}dt - \int_0^t X_{RL}dt\right] \to 0 \tag{7}$$

Substituting the expression of X_{RS} from Eqn. (6) into Eqn. (7), and normalizing it with respect to $X_{RL} = 1(t)$, yields to the following integral:

$$-e_{ramp} = \int_0^{\infty} -\exp^{-\sigma t}\left[\cos\omega_d t + \frac{\sigma}{\omega_d}\sin\omega_d t\right]dt \tag{8}$$

Solving the integral yields:

$$-e_{ramp} = -\left[\frac{\sigma}{\omega_d^2+\sigma^2} + \frac{\sigma}{\omega_d}\frac{\omega_d}{\omega_d^2+\sigma^2}\right] \implies e_{ramp} = \frac{2\zeta}{\omega_n} \tag{9}$$

The result from Eqn. (9) shows that, for a pure second order dynamic, area-matching can be only ensured if $\omega_n = \infty$ or the system is undamped, i.e. $\zeta = 0$. Such an undamped system which exhibits a sinusoidal step response, is not appropriate for realistic applications such as power systems. In addition, for non ideal cases of $\eta < 1$, Eqn. (4) requires that the $\sum_{j=1}^{\infty} A_{a,j}$ be greater than $\sum_{j=1}^{\infty} A_{b,i}$, $\eta = \frac{\sum_{j=1}^{\infty} A_{b,i}}{\sum_{j=1}^{\infty} A_{a,j}}$. This can be achieved by having a system with a negative e_{ramp} which is not feasible in systems with a pure second order dynamic.

2.1 Effect of Zero Placement

In the previous section, it was shown that a system with a pure second order dynamic does not satisfy the condition of the area-matching that is stated in Eqn. (4). Increasing the order of the system represents an alternate path to be explored ; however, as a result, the system will be more complicated. One of the effective methods to modify response characteristics of systems and at the same time preserve the order, is the minimum phase zeros placement approach. An additional zero with a certain location can significantly influence the response of the system through increasing its overshoot. Moreover, the presence of a proper zero in the system can substantially enhance the steady state response and guarantee minimum or zero error in following the input signal. Therefore, a modified second order system with an additional zero is investigated.

Consider adding a zero with a value of α to Eqn. (5) as follow:

$$\ddot{X} + 2\zeta\omega_n \dot{X} + {\omega_n}^2 X = {\omega_n}^2 u(t) + \alpha\dot{u}(t) \tag{10}$$

To find the step response, Eqn. (10) is first transformed to the frequency domain as shown below:

$$\frac{X(s)}{u(s)} = \bar{G}(s) = \frac{\omega_n^2 + \alpha s}{s^2 + 2\zeta\omega_n s + \omega_n^2} \tag{11}$$

The Laplace inverse of Eqn. (11) produces

$$X(t) = 1 - \exp^{-\sigma t}\left[\cos\omega_d t + \frac{\sigma-\alpha}{\omega_d}\sin\omega_d t\right] \tag{12}$$

Applying Eqn. (12) into Eqn. (7) with $X_{RS} = X(t)$ and $X_{RL} = 1(t)$, leads to the following result:

$$-e_{ramp} = -[\frac{\sigma}{\omega_d^2+\sigma^2} + \frac{\sigma-\alpha}{\omega_d}\frac{\omega_d}{\omega_d^2+\sigma^2}] = \frac{\alpha - 2\zeta\omega_n}{\omega_n^2} \tag{13}$$

The necessary condition of stability requires that the coefficient $2\zeta\omega_n$ to be positive. In Eqn. (13) setting $\alpha = 2\zeta\omega_n$ returns a zero e_{ramp}. Similarly, using $0 < \alpha < 2\zeta\omega_n$ and $\alpha > 2\zeta\omega_n$ produce a positive and negative e_{ramp}, respectively. Consequently, area-matching is feasible for a modified second order dynamic if a proper zero, $\alpha \geq 2\zeta\omega_n$, is added to the system. Hence, for the ideal case of $\eta = 1$, the proper value of α that ensures area-matching equals $2\zeta\omega_n$. However, for non ideal cases $\eta \leq 1$, the analysis is not explicit. Therefore, the analysis of finding the location of the proper zero for a given value of $[\eta = \frac{\sum_{j=1}^{\infty} A_{b,i}}{\sum_{j=1}^{\infty} A_{a,j}}] < 1$ is discussed in the next section.

2.2 An Infinite Analysis to Relate the Efficiency η with the Zero Location

The condition to maintain area-matching with the presence of η is stated in Eqn. (4). Utilizing the result of Eqn. (13) from

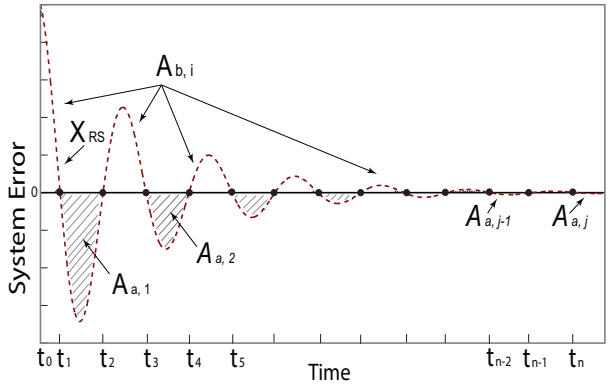

FIGURE 2. GEOMETRIC SERIES ANALYSIS.

the previous section, Eqn. (4) can be modified as follow:

$$A_{RS} - A_{RL} = [1-\eta]\sum_{j}^{\infty} A_{a,j} = -e_{ramp} = \frac{\alpha - 2\zeta\omega_n}{\omega_n^2} \tag{14}$$

Similar to the ideal case, a proper zero α that can ensure the applicability of area-matching must be found. Eqn. (14) includes two unknowns that are required to obtain α. These are $\sum_{j=1}^{\infty} A_{a,j}$ and η. Therefore, the method of finding α for a given η is addressed below. Using this approach requires knowing the total value of $\sum_{j=1}^{\infty} A_{a,j}$ when the dynamic response of the system converges to a steady state.

Referring to Fig. 2, one can conjecture that the areas of the shown response with respect to the reference line of a step signal follows a specific progression. Therefore, a geometric series analysis is utilized to validate this resemblance argument and evaluate $\sum_{j=1}^{\infty} A_{a,j}$. First, Eqn. (12) is rearranged as

$$X(t) = 1 - \exp^{-\sigma t}\beta\,[\sin(\omega_d t + \phi)] \tag{15}$$

where $\beta = \sqrt{1+\gamma^2}$, $\gamma = \frac{\sigma-\alpha}{\omega_d}$ and ϕ is the phase angle . Then, the step error of Eqn. (15) is

$$X(t) = \exp^{-\sigma t}\beta\,[\sin(\omega_d t + \phi)] \tag{16}$$

Subsequently, Eqn. (16) is integrated for the interval $t_n \rightarrow t_{n+1}, n = 1,2,...$ which yields:

$$A_{a,j} = \frac{-\beta}{\sigma^2+\omega_d^2}\exp^{-\sigma t_n}[\sigma\sin(\omega_d t_n+\phi) + \omega_d\cos(\omega_d t_n+\phi)]_{t_{n=2j-1}}^{t_{n=2j}} \tag{17}$$

In order to utilize the result from Eqn. (17), integration intervals t_n, $n = 0,1,2,...$ are evaluated through finding the roots of Eqn. (15) at $\sin(\omega_d t + \phi) = 0$ i.e. the roots at:

$$(\omega_d t_n + \phi) = n\pi, n = 0,1,2,... \tag{18}$$

which leads to:

$$t_n = \frac{n\pi - \phi}{\omega_d}, n = 1,2,... \tag{19}$$

Thus, the values of areas $A_{a,j}$, $j = 1,2,3,...$ can be obtained using:

$$A_{a,j} = \frac{-\beta\,\omega_d}{\sigma^2+\omega_d^2}\left[\exp^{-\sigma\frac{(2j)\pi-\phi}{\omega_d}} + \exp^{-\sigma\frac{(2j-1)\pi-\phi}{\omega_d}}\right] \tag{20}$$

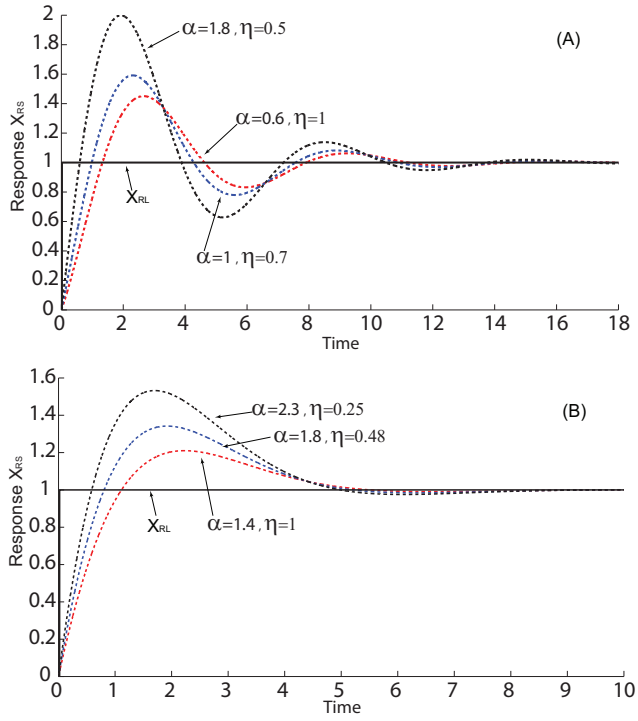

FIGURE 3. RESPONSE WITH DIFFERENT VALUES OF α FOR: (A) $\zeta = 0.3$, (B) $\zeta = 0.7$.

Next, in order to evaluate $\sum_{j=1}^{\infty} A_{a,j}$ using geometric series analysis, the ratio r between each two successive terms must be constant, which is indeed the case as shown in the result below:

$$r = \frac{A_{a,j+1}}{A_{a,j}} = \exp^{-\frac{2\pi\sigma}{\omega_d}}, j = 1,2,3,... \tag{21}$$

The definition of geometric series is then used to find the value at which $\sum_{j=1}^{\infty} A_{a,j}$ converges as follows [16]:

$$\sum_{j=1}^{\infty} A_{a,j} = \sum_{j=1}^{\infty} A_{a,1} r^{(j-1)} = \frac{A_{a,1}}{1-r}, |\,r\,| < 1. \tag{22}$$

where r is defined in Eqn. (21), and $A_{a,1}$ can be found from Eqn. (20) as:

$$A_{a,1} = \frac{-\beta\,\omega_d}{\sigma^2+\omega_d^2}\left[\exp^{-\sigma\frac{2\pi-\phi}{\omega_d}} + \exp^{-\sigma\frac{\pi-\phi}{\omega_d}}\right] \tag{23}$$

Finally, by substituting the result from Eqn. (22) into Eqn. (14), the efficiency η can be expressed as:

$$\eta = 1 - \frac{(1-r)[\alpha - 2\zeta\,\omega_n]}{\omega_n^2 A_{a,1}} = 1 + \frac{(1-r)\,e_{ramp}}{A_{a,1}} \tag{24}$$

Although Eqn. (24) does not provide an explicit expression for α , it can be utilized numerically to define a range of values by which a proper zero for a desired η can be located.

3 OBSERVATIONS

3.1 System Characteristics

Simulation results to validate the analysis of area-matching are presented in Fig. 3 and Fig. 4. In all the simulation scenarios, the natural frequency was chosen to be $\omega_n = 1 rad/sec$ while

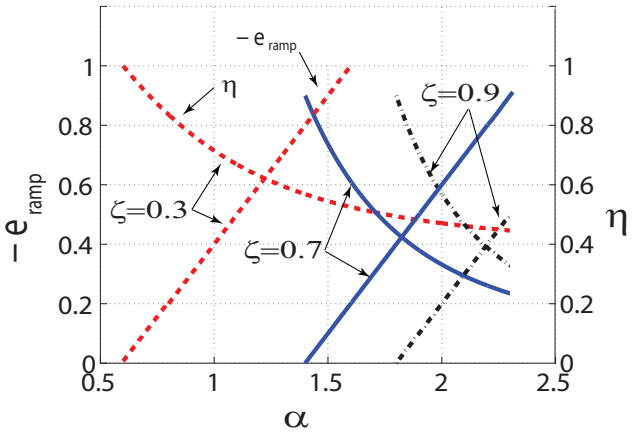

FIGURE 4. SYSTEM RAMP ERROR AND η VS. α with $\omega_n = 1$.

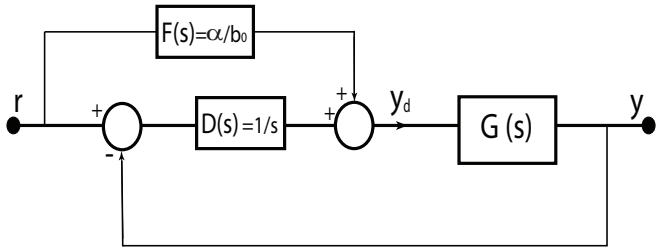

FIGURE 5. FEEDBACK AND FEEDFORWARD SCHEMATIC.

different values of the damping ratio ζ were selected. Fig. 3 shows the response X_{RS} using different values of system zero α. In Fig. 3 (A), the damping ratio is set to be $\zeta = 0.3$. On the other hand, in Fig. 3 (B), the damping ratio is set to be $\zeta = 0.7$ which provides low oscillation behavior; thus cycling will be minimized which is desired in realistic applications such as power systems. The curves with $\alpha = 0.6$ and $\alpha = 1.4$ represent the ideal case ($\eta = 1$) for $\zeta = 0.3$ and $\zeta = 0.7$, respectively, while the other curves represent the non ideal case where η is less than unity. As seen from Fig. 3, by changing the value of α, the areas $A_{a,l}$ will be proportionally affected. Increasing α will increase the areas $A_{a,j}$ and decreases the areas $A_{b,i}$. Hence, $\eta = \frac{\sum_{j=1}^{\infty} A_{b,i}}{\sum_{j=1}^{\infty} A_{a,j}}$ will be affected. This observation is also confirmed in Fig. 4 which presents the relation between η and the system zero α. The condition, $e_{ramp} \leq 0$ which is required to get $\eta \leq 1$ is also confirmed in Fig. 4 where three different values of $\zeta = 0.3, 0.7$, and 0.9 were used.

3.2 Realization with Feedback and Feedforward Control

One of the main aspects of this research investigation was to answer the following question : What kind of system can provide a response that ensures the applicability of the area-matching ? This inquiry has been clarified in the aforementioned analysis and it has been shown that a system with a transfer function that is equivalent to the one stated in Eqn. (11), achieves the task. The transfer function of systems can take different forms of first or second order or even higher. For instance, if the given transfer function represents a first order system, then the order of the system has to be increased. On the other hand, if the given transfer function represents a second order system, then the controller has to modify the system without increasing its order. One approach might be changing the type of the system from type one to type two. To illustrate this, without any loss of generality, consider given a first order transfer function with a D.C. gain =1. Ideally when system $\eta = 1$, the area matching approach requires that $e_{ramp} = 0$ and this can be achieved by adding an integral block in the feedback loop of the transfer function. However, changing the type of the system will not provide a remedy to non ideal cases where the e_{ramp} is required to be negative. Therefore, the control strategy has to have the ability to place a proper zero, yet maintain the required order of the system. Consequently, feedforward and feedback actions should be implemented on the system as required to achieve the form of the transfer function from Eqn. (11). Fig. 5 shows an example to illustrate this idea. Consider given a strictly proper first order transfer function as shown in Eqn. (25):

$$T.F. = G(s) = \frac{b_0}{s + a_0} \tag{25}$$

the order of the system has to be increased to a second order using an integrator block. In addition, a proper zero has to be placed using the feedforward loop. Hence, to have a transfer function that matches Eqn. (11), the gains $F(s)$ and $D(s)$ in Fig. 5 can be set to $\frac{\alpha}{b_0}$ and $\frac{1}{s}$, respectively, which produces

$$\bar{G}(s) = \frac{G(s)[D(s) + F(s)]}{1 + D(s)G(s)} = \frac{b_0 + \alpha s}{s^2 + a_0 s + b_0} \tag{26}$$

with $a_0 = 2\zeta\omega_n$ and $b_0 = \omega_n^2$. Similarly, for the case of being given a strictly proper second order system with no zero, the only modification would be to add a feedforward gain to place the required zero and preserve the system order. It can be seen from the above example that the addition of zero is determined by the controllers $F(s)$ and $D(s)$, and not by the planet transfer function $G(s)$. Furthermore, it can be analyzed and shown that if the relative degree of the controller $D(s)$ is (≥ 1), (e.g. the integral controller $\frac{1}{s}$) then the additional zero will be introduced to the system. However, when the relative degree of the controller $D(s)$ is *zero* (e.g. PI controller: $\frac{cs+d}{s}$) the affect of the controller $F(s)$ is to change the location of the original zero without adding additional zero to the system.

3.3 Higher Order System Analysis

In this section, extending the analysis of area-matching to be applied for higher order system is discussed. Consider the close loop transfer function of the block diagram presented in Fig. 5

$$\bar{G}(s) = \frac{G(s)[D(s) + F(s)]}{1 + D(s)G(s)} \tag{27}$$

Assuming that the $D.C.gain of \bar{G}(s) = 1$ then the e_{ramp} can be obtained as:

$$e_{ramp} = \lim_{s\to 0}\left[\frac{1}{s^2} - \frac{\bar{G}(s)}{s^2}\right] s = \lim_{s\to 0}\left[\frac{1-\bar{G}(s)}{s}\right] = \lim_{s\to 0}\bar{G}'(s) \quad (28)$$

where $\bar{G}'(s) = \frac{d}{ds}\bar{G}(s)$. Consequently, a general outcome of this analysis is that for any system with a D.C. gain of 1 , e_{ramp} can be predicted by tacking the derivative of the closed loop transfer function with respect to s and setting it to *zero*,

Next, consider given a higher order transfer function that is rational and strictly proper, and has a D.C. gain of 1.

$$\bar{G}(s) = \frac{N(s)}{D(s)} = \frac{n(s)+k_n s+k_0}{d(s)+k_d s+k_0} \quad (29)$$

By using the result from Eqn. (28), it can be shown that

$$e_{ramp} = \lim_{s\to 0}\frac{d}{ds}\left(\frac{N(s)}{D(s)}\right) = \frac{k_d - k_n}{k_0} \quad (30)$$

The result from Eqn. (30) can be compared with

$$e_{ramp} = \frac{2\zeta\omega_n - \alpha}{\omega_n^2} \quad (31)$$

with $k_d = 2\zeta\omega_n$, $k_n = \alpha$, and $k_0 = \omega_n^2$. Eqn. (30) represents a generalized result for rational-polynomial transfer functions, and shows that the location of a proper zero can be predicted by examining the parameters k_n, k_d, and k_0.

CONCLUSION

The idea of shaping a transient response of dynamic systems using minimum phase zeros is explored. The goal is to determine the zero locations that satisfy a conservation principle. It is shown that such characteristic is infeasible for first order and second order systems with no additional zero. The simplest dynamic system where this area matching can be achieved is a second order system with an additional zero. In this regard, it is shown that a combination of feedback and feedforward actions can place/add a proper zero at an appropriate location. Through a geometric series analysis, we analytically find a relation between the zero location and the corresponding area mismatch. In hybrid power systems, this refers to achieving a certain efficiency of power transmission from the power source to the energy storage. Other potential applications could be in the rendezvous / pursuit problems. Future work in this would include an extension and development of a rigorous theory for general transfer functions, a part of which has been initiated in this work. Further development to nonlinear dynamical systems is also feasible.

REFERENCES

[1] Barley, C. D., and Winn, C. B., 1996. "Optimal dispatch strategy in remote hybrid power systems". *Solar Energy,* ***58***(4-6), pp. 165–179.

[2] Paska, J., Biczel, P., and Kłos, M., 2009. "Hybrid power systems–an effective way of utilising primary energy sources". *Renewable Energy,* ***34***(11), pp. 2414–2421.

[3] Barley, C. D., and Winn, C. B., 1997. "Remote hybrid power systems". *Advances in solar energy,* ***11***.

[4] Nehrir, M., Wang, C., Strunz, K., Aki, H., Ramakumar, R., Bing, J., Miao, Z., and Salameh, Z., 2011. "A review of hybrid renewable/alternative energy systems for electric power generation: Configurations, control, and applications". *IEEE Transactions on Sustainable Energy,* ***2***(4), pp. 392–403.

[5] Chu, A., and Braatz, P., 2002. "Comparison of commercial supercapacitors and high-power lithium-ion batteries for power-assist applications in hybrid electric vehicles: I. initial characterization". *Journal of power sources,* ***112***(1), pp. 236–246.

[6] Das, T., Narayanan, S., and Mukherjee, R., 2010. "Steady-state and transient analysis of a steam-reformer based solid oxide fuel cell system". *Journal of Fuel Cell Science and Technology,* ***7***(1), p. 011022.

[7] Allag, T., and Das, T., 2012. "Robust control of solid oxide fuel cell ultracapacitor hybrid system". *IEEE transactions on control systems technology,* ***20***(1), pp. 1–10.

[8] Vahidi, A., and Greenwell, W., 2007. "A decentralized model predictive control approach to power management of a fuel cell-ultracapacitor hybrid". In American Control Conference, 2007. ACC'07, IEEE, pp. 5431–5437.

[9] Bakule, L., 2008. "Decentralized control: An overview". *Annual reviews in control,* ***32***(1), pp. 87–98.

[10] Ugrinovskii*, V., and Pota, H. R., 2005. "Decentralized control of power systems via robust control of uncertain markov jump parameter systems". *International Journal of Control,* ***78***(9), pp. 662–677.

[11] Sendjaja, A. Y., and Kariwala, V., 2011. "Decentralized control of solid oxide fuel cells". *IEEE Transactions on Industrial Informatics,* ***7***(2), pp. 163–170.

[12] Madani, O., Bhattacharjee, A., and Das, T., 2016. "Decentralized power management in a hybrid fuel cell ultracapacitor system". *IEEE Transactions on Control Systems Technology,* ***24***(3), pp. 765–778.

[13] Llamas, A., and De La Ree, J., 1993. "Stability and the transient energy method for the classroom". In System Theory, 1993. Proceedings SSST'93., Twenty-Fifth Southeastern Symposium on, IEEE, pp. 79–85.

[14] Amin, M., and Aqilah, N., 2013. "Power system transient stability analysis using matlab software". PhD thesis, Universiti Tun Hussein Onn Malaysia.

[15] Fang, L., and Ji-Lai, Y., 2009. "Transient stability analysis with equal area criterion directly used to a non-equivalent generator pair". In Power Engineering, Energy and Electrical Drives, 2009. POWERENG'09. International Conference on, IEEE, pp. 386–389.

[16] Andrews, G. E., 1998. "The geometric series in calculus". *The American mathematical monthly,* ***105***(1), pp. 36–40.